$(1s)^4\ 2\sigma_g^2\ 2\sigma_u^{*2}\ 3\sigma_g^2\ 1\pi_u^4$

HF Korr. pályasorrend

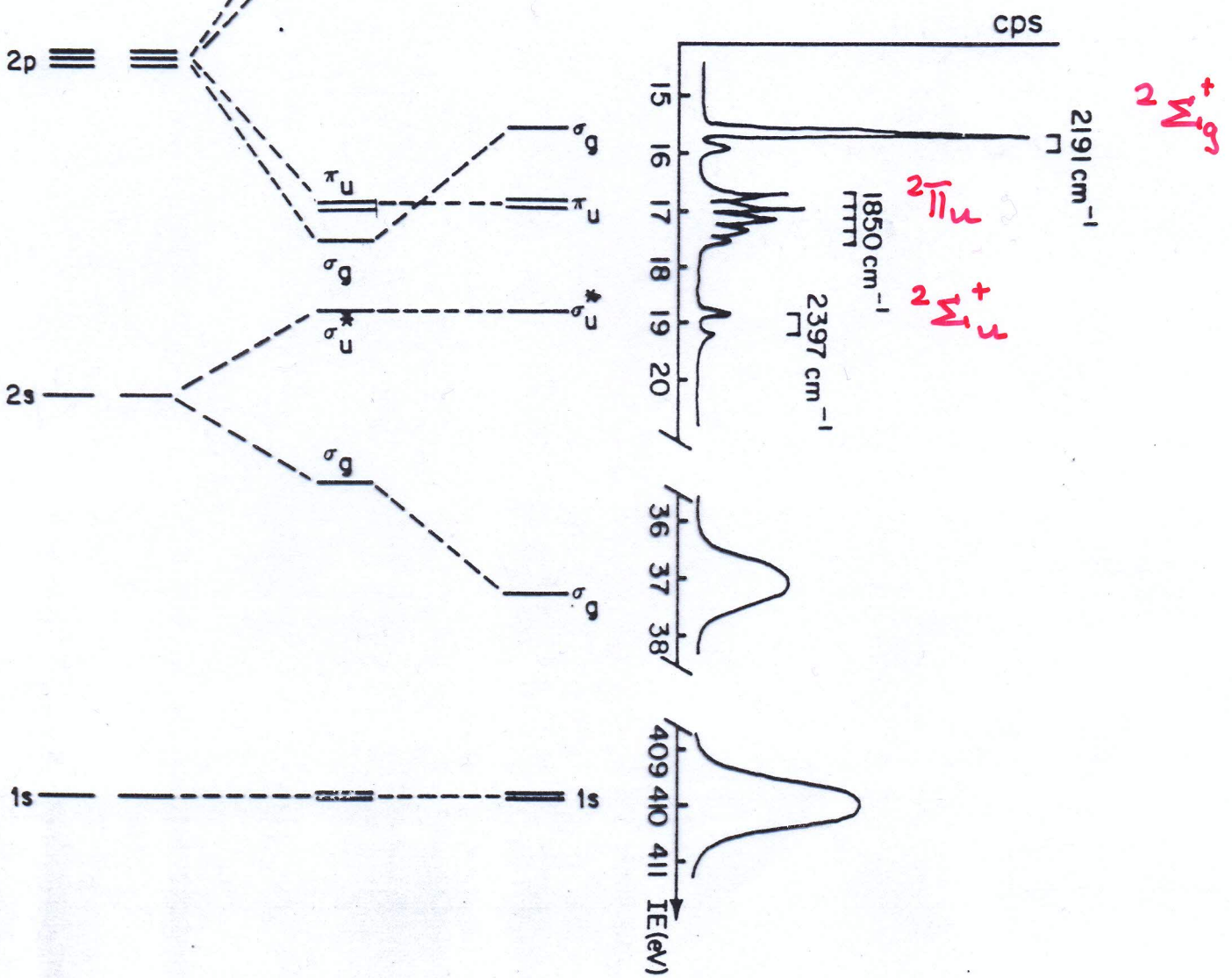

Figure 5. Nitrogen molecule comparison of qualitative MO scheme with the photoelectron spectrum.

$\nu\ (N-N) = 2360\ cm^{-1}$

Spin-pálya kölcsönhatás

Ha egy zárthéjú rendszer (atom, molekula) degenerált alhéjáról történik ionizáció, akkor a spin- és pálya impulzusmomentum kölcsönhatásának eredményeképp spin-pálya csatolás lép fel, vagyis az egy pályához tartozó sáv felhasad.
[$^2\Gamma$ állapot, $(\gamma)^{2\omega-1}$ elektron konfiguráció, γ – szimmetria, ω – az alhéj degeneráltsága.]

$$E_{SO} = -(\zeta/\hbar^2)\, \mathbf{L}\cdot\mathbf{S}$$

ahol **L** és **S** a pálya- és spin impulzusmomentum vektora, ζ a SO csatolási állandó.

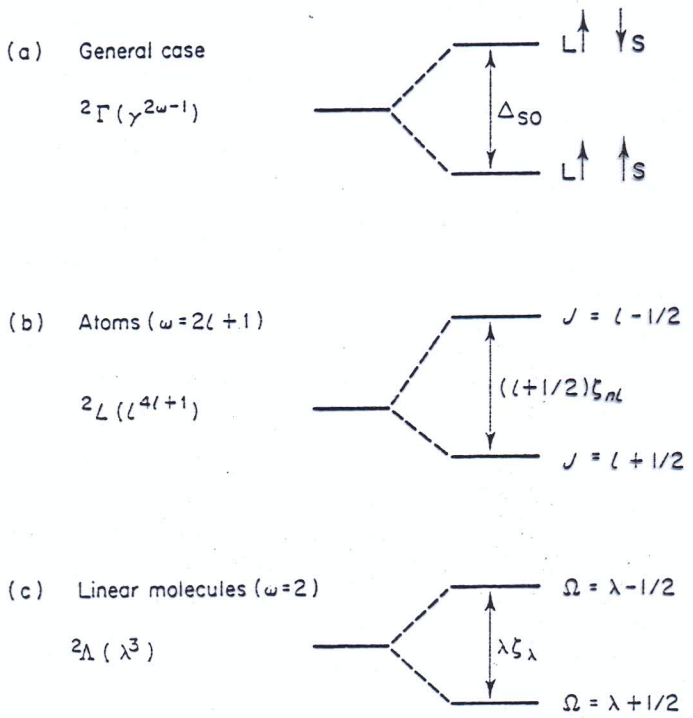

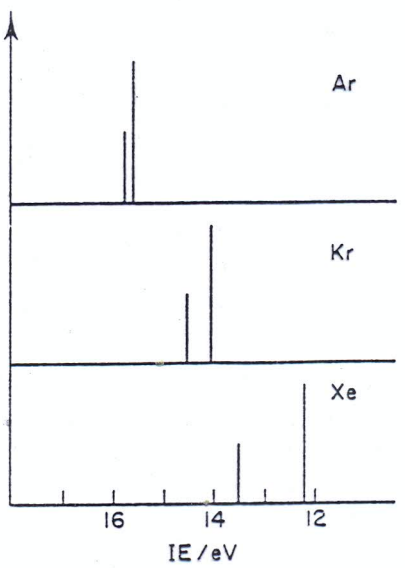

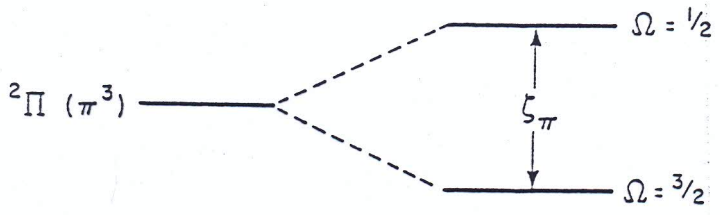
$^2\Pi$ (π^3)
$\Omega = 1/2$
ζ_π
$\Omega = 3/2$

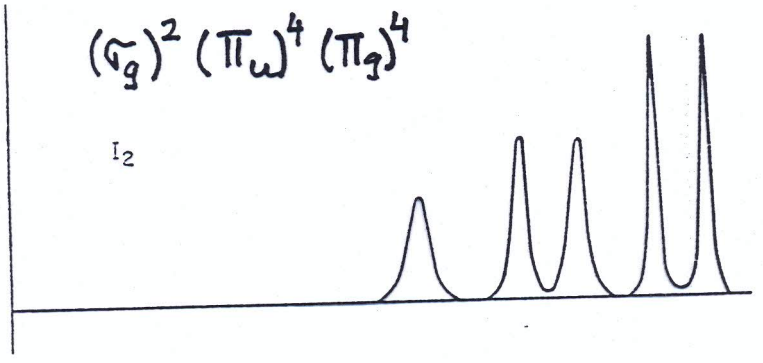
$(\sigma_g)^2 (\pi_u)^4 (\pi_g)^4$
I_2

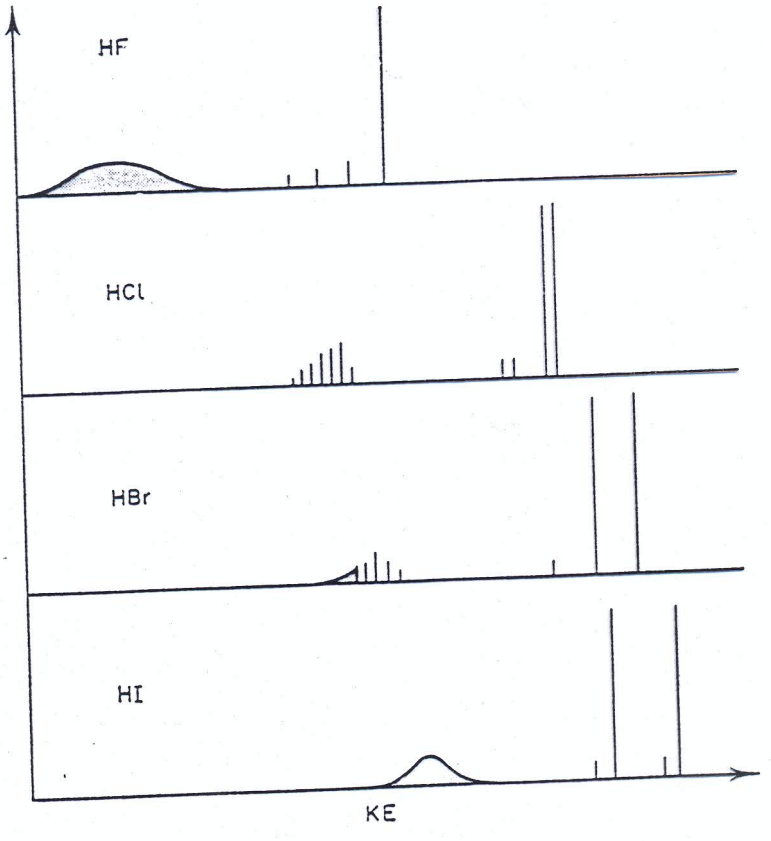
HF
HCl
HBr
HI
KE

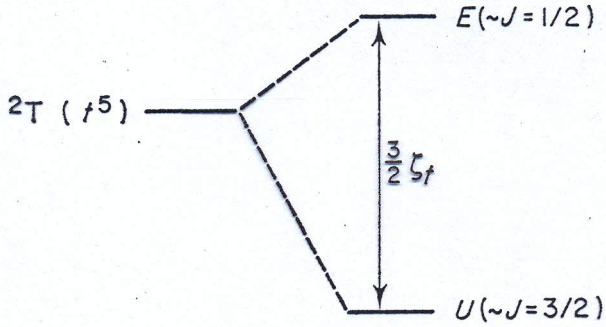

Fig. 21. The splitting under spin-orbit coupling of a $^2T(t^5)$ level in a cubic molecule. ζ_t is the spin-orbit coupling constant of the t sub-shell involved. The splitting resembles that which occurs in ^2P states of atoms (cf. Fig. 18b).

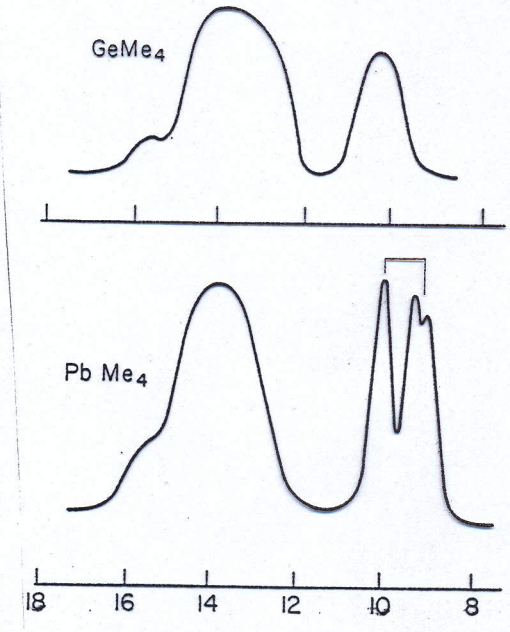

$$P_{FC}(0, v') = \left|\int \psi_0 \psi_v^+, \mathrm{d}x\right|^2$$

i.e. the square of the overlap integral between the vibrational wave functions in the initial and final states. The sum $\sum P_{FC}(0, v')$ of the individual Franck–Condon factors equals the overall probability P of the photoionization process in question.

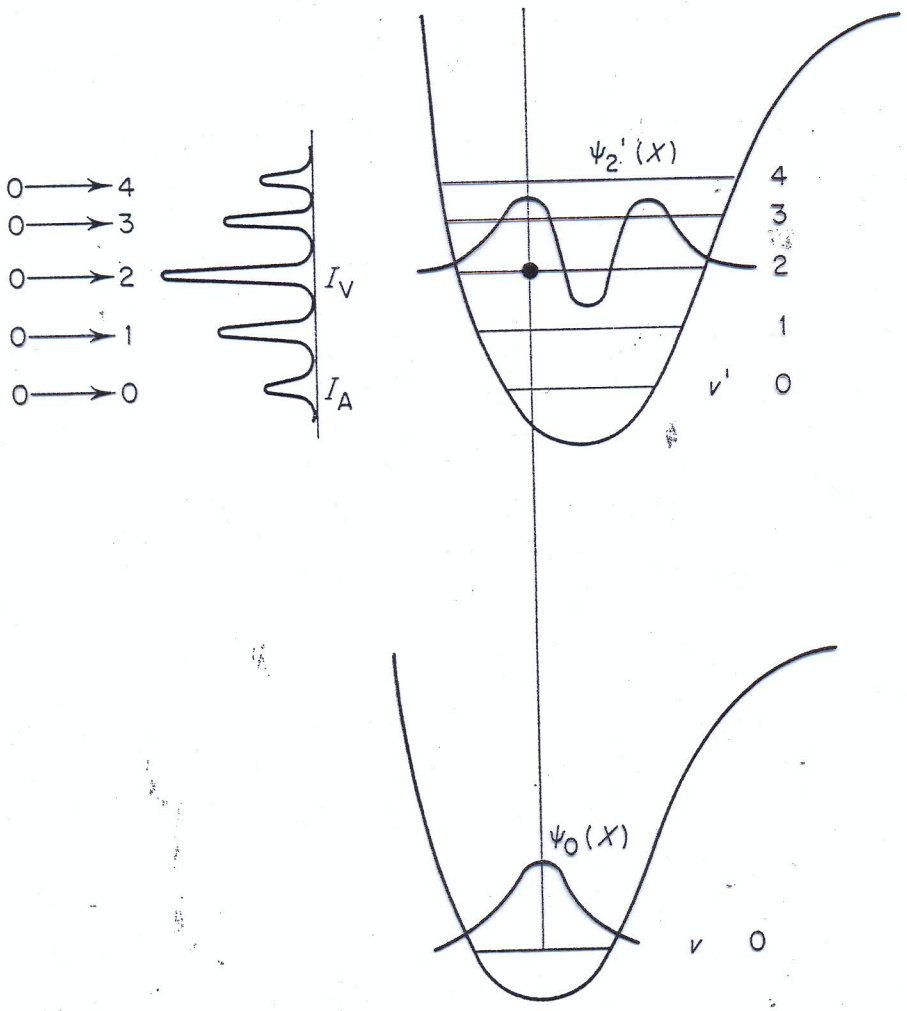

Fig. 24. Potential energy curves for a molecule and one of its ionized states, illustrating the 'vertical' nature of the photoionization process and the production of the molecule-ion in different vibrational states.

	HF	HCl	HBr	HI
ν_π		2680	2420	2100
ν_σ		1610	1290	1300
ν_0	4140	2990	2560	2230

The spin-orbit coupling constants ζ_π for the $\pi(\mathrm{X}np_\pi)$ orbitals compared with the f
parameters ζ_{np}.

	HF	HCl	HBr	HI
ζ_π	240	640	2660	4300
	F	Cl	Br	I
ζ_{np}	270	590	2460	5070

$1\ \mathrm{cm}^{-1} = 1.240 \times 10^{-4}$ eV *or* 1.986×10^{-23} J.

HCl [Cl 3s]$^2\sigma^2\ ^2\pi^4_{Cl}$

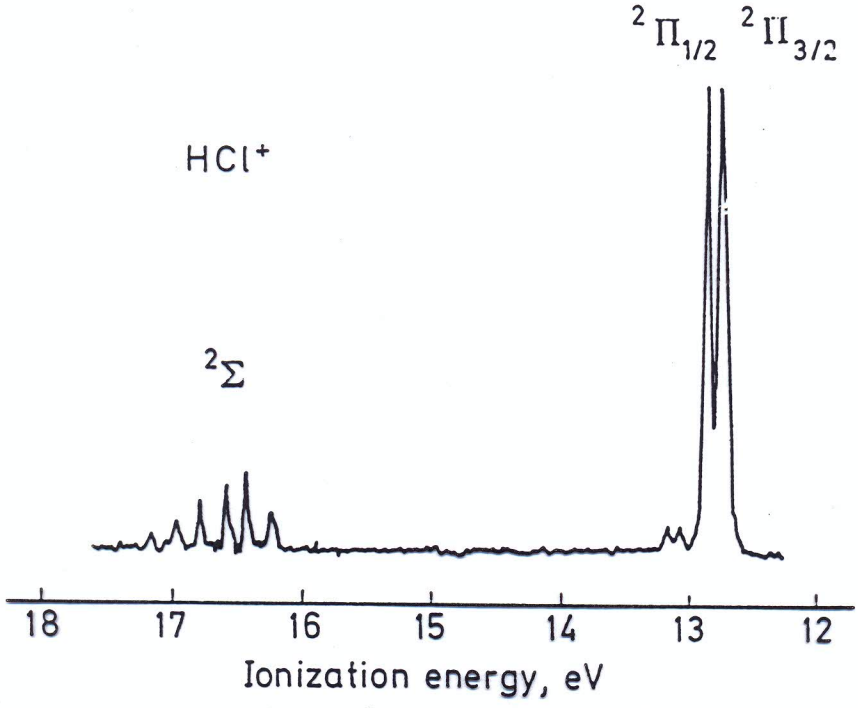

Figure 6.1. Photoelectron spectrum of HCl ionized by He I light

I_2 [...] $\sigma_g^2\ \sigma_u^{*2}\ \sigma_g^2\ \pi_u^4\ \pi_g^{*4}$

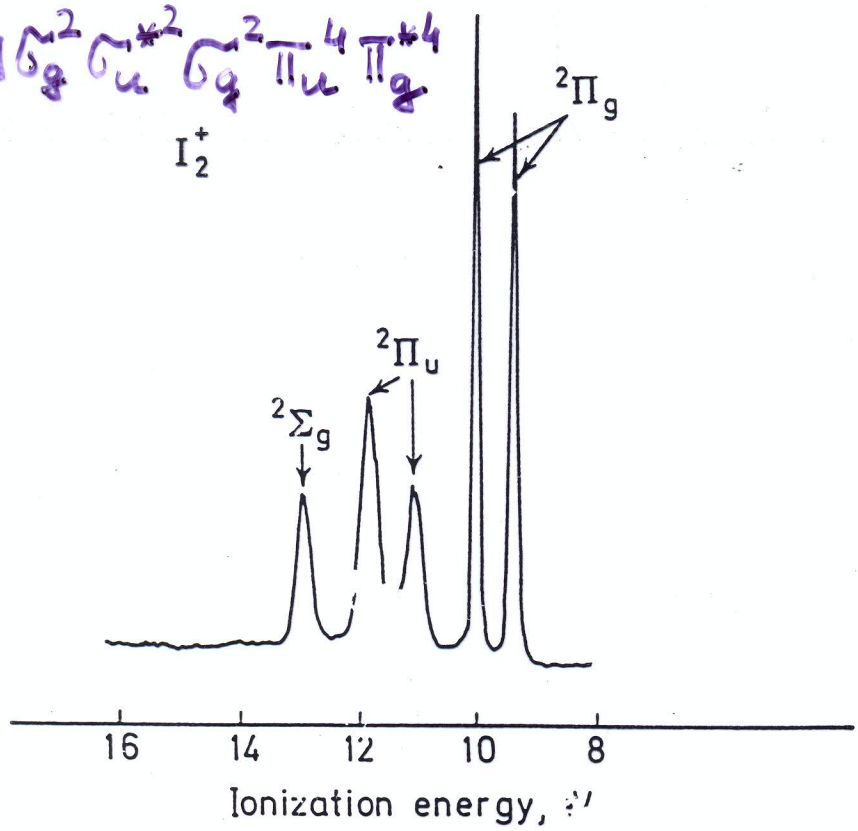

Figure 6.2. Photoelectron spectrum of iodine showing spin-orbit splitting in the $^2\Pi_g$ and $^2\Pi_u$ ionic states. (From Evans, S. and Orchard, A. F., *Inorg. Chim. Acta*, 5, 81 (1971), by permission)

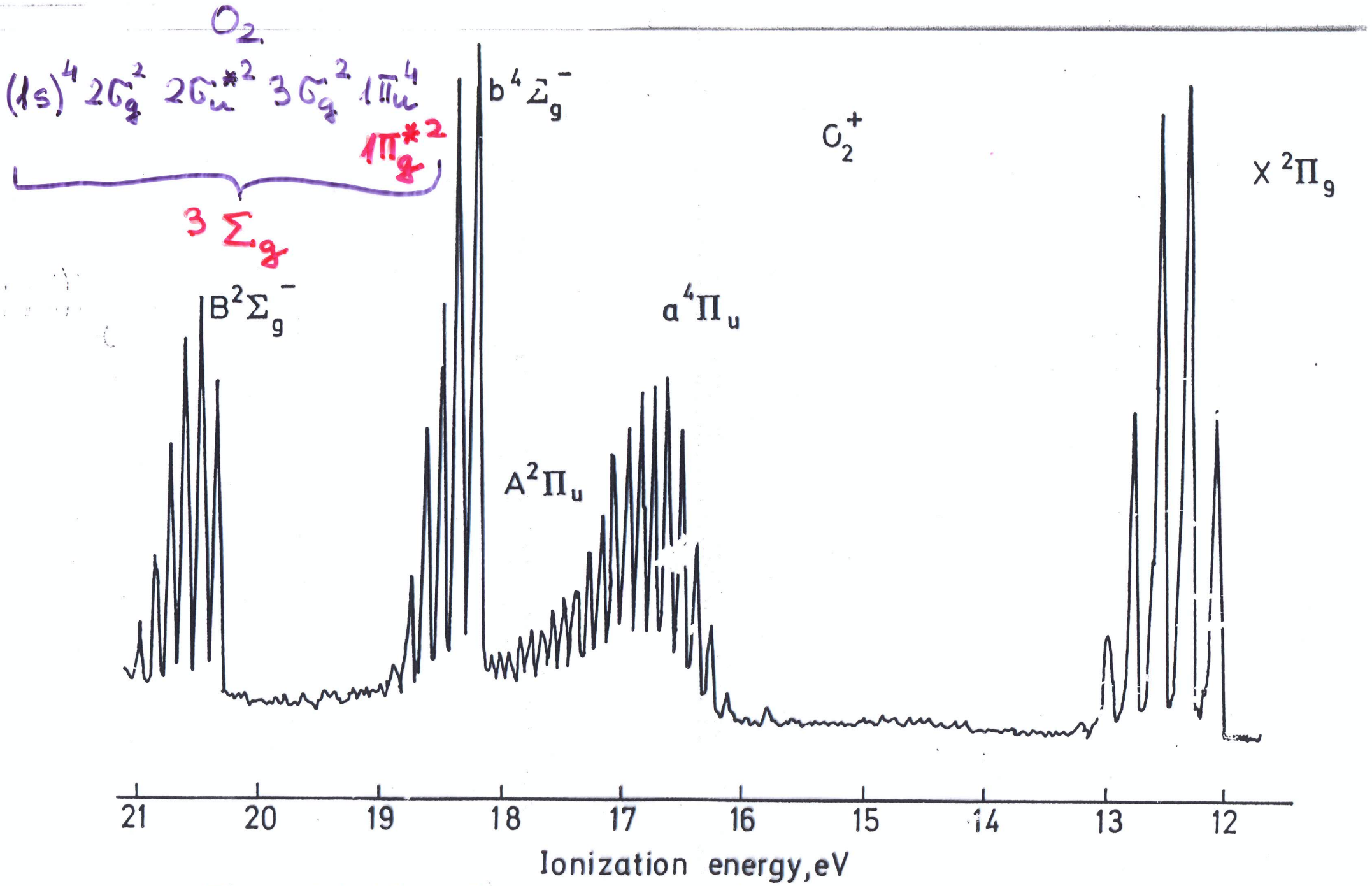

Figure 1.6. Photoelectron spectrum of oxygen excited by He I radiation

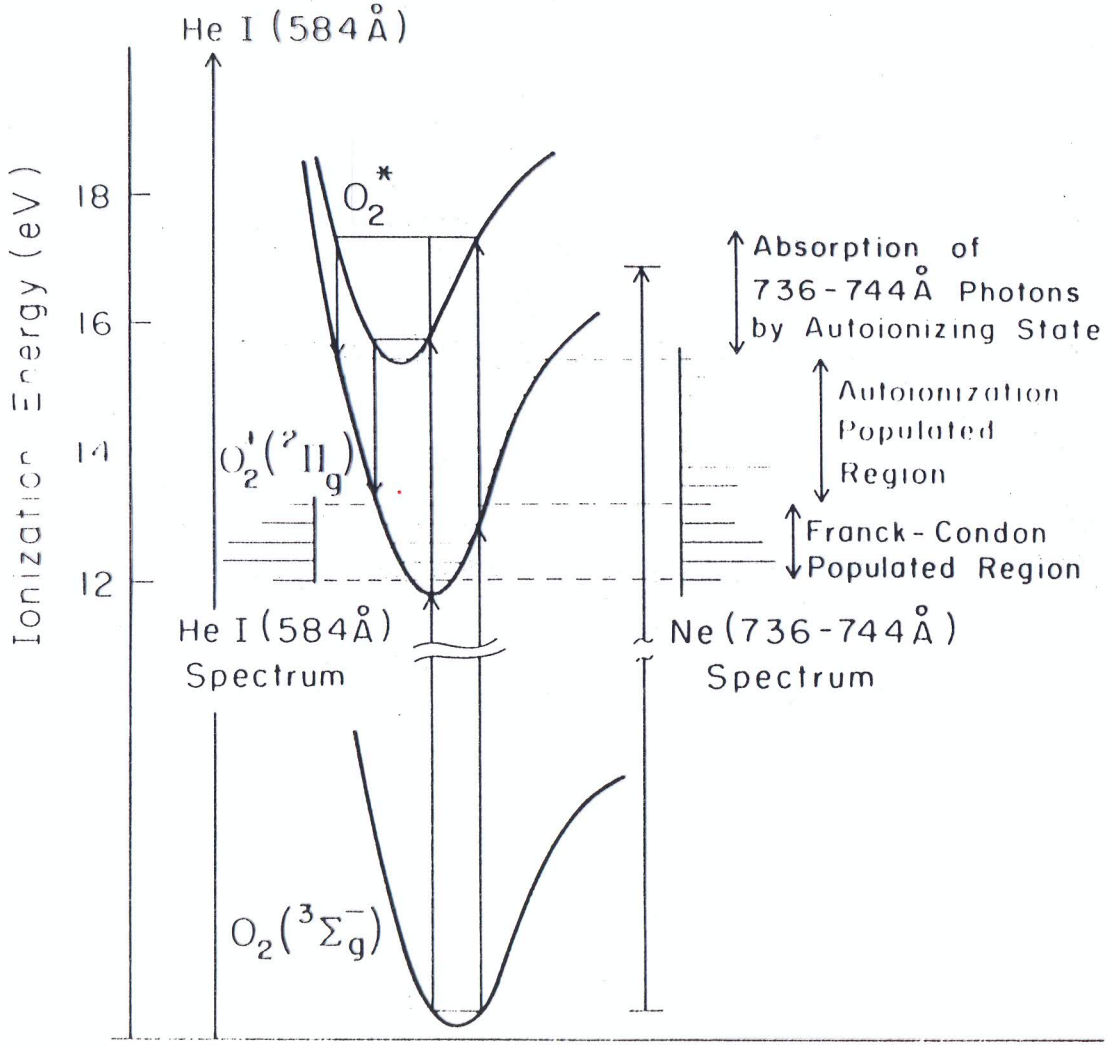

Fig. 3.12. Schematic diagram representing direct and autoionizing transitions of O_2.

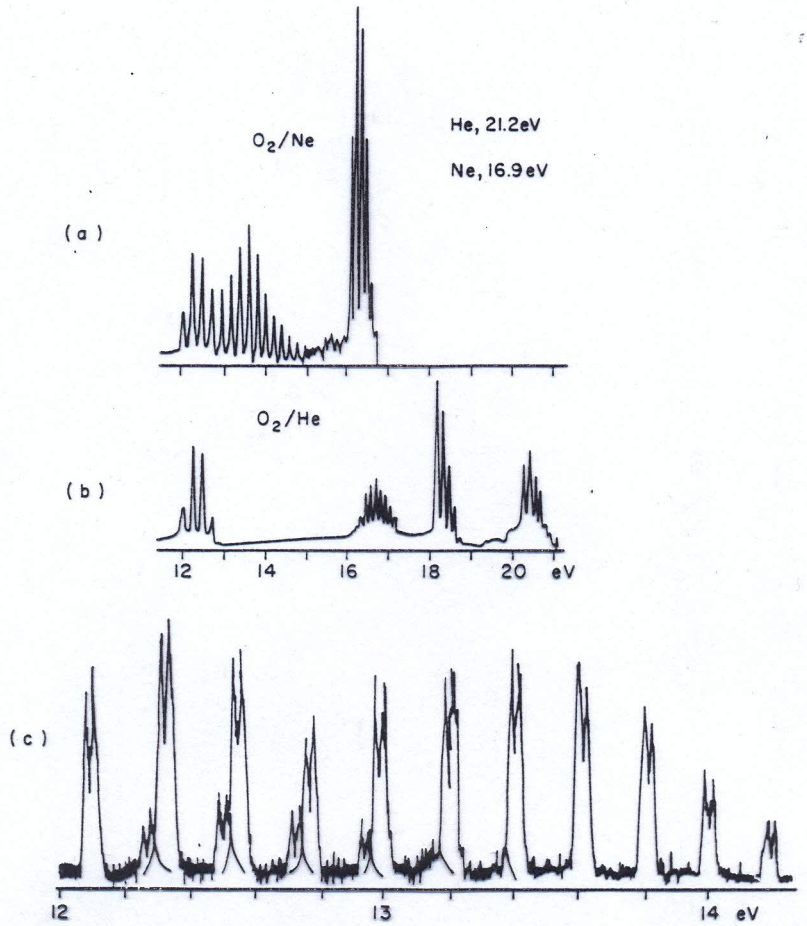

Fig. 25. (a) Photoelectron spectrum of O_2 taken with Ne I radiation. (b) Photoelectron spectrum of O_2 taken with He I radiation. (c) High resolution spectrum of O_2 using Ne I radiation showing autoionization enhancement by the 16·85 eV line (major peaks) but not by the 16·67 eV line (minor peaks).

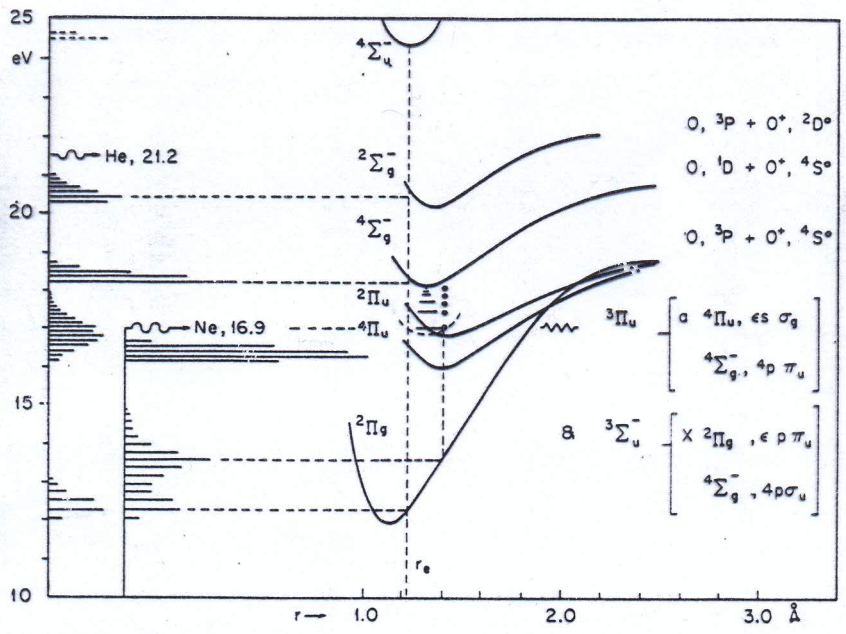

Fig. 27. Potential energy curves of O_2^+ with photoelectron spectrum drawn along the ordinate indicating the nature of the autoionizing processes.

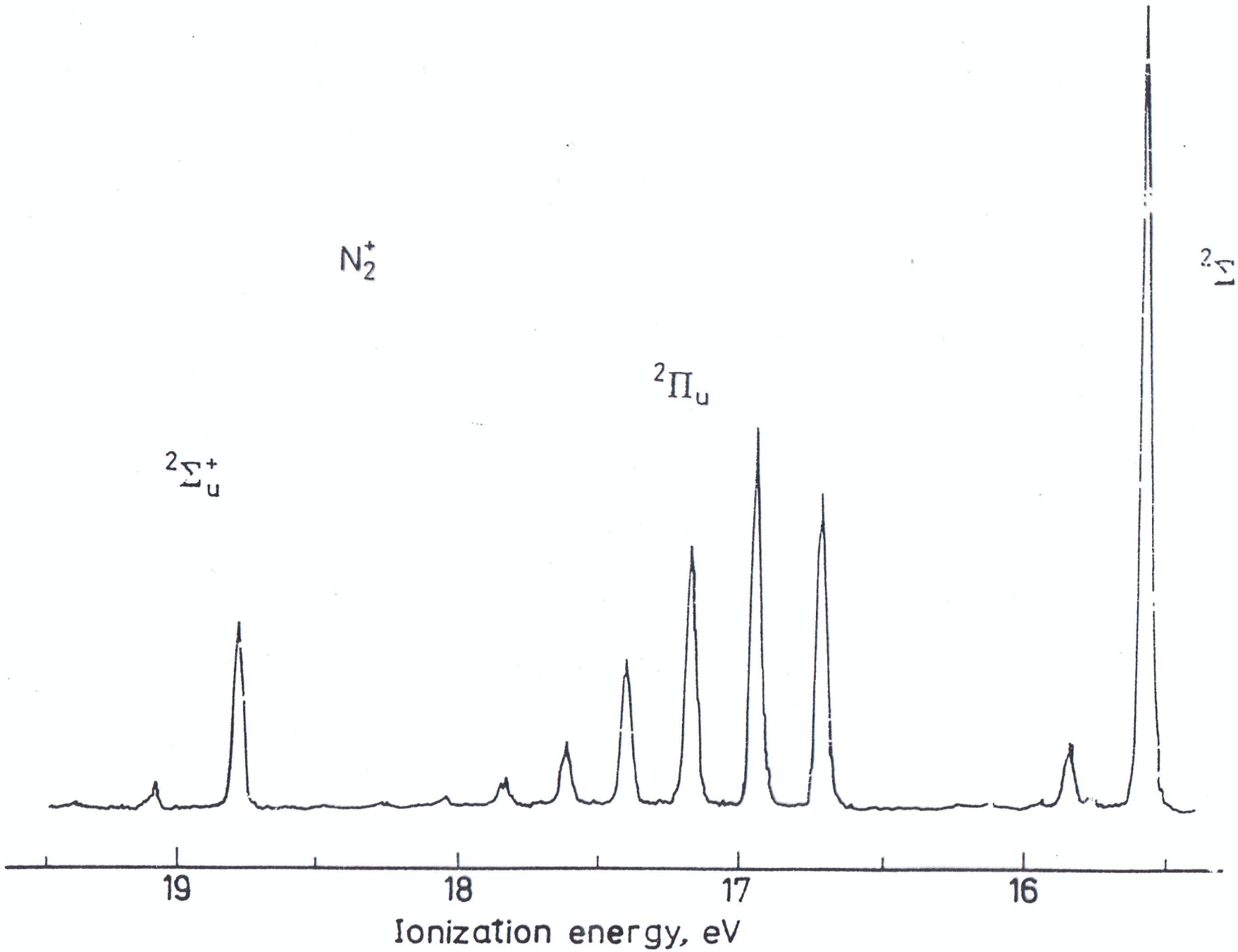

Figure 1.4. Photoelectron spectrum of nitrogen excited by He I radiation. (By courtesy of Professor W. C. Price)

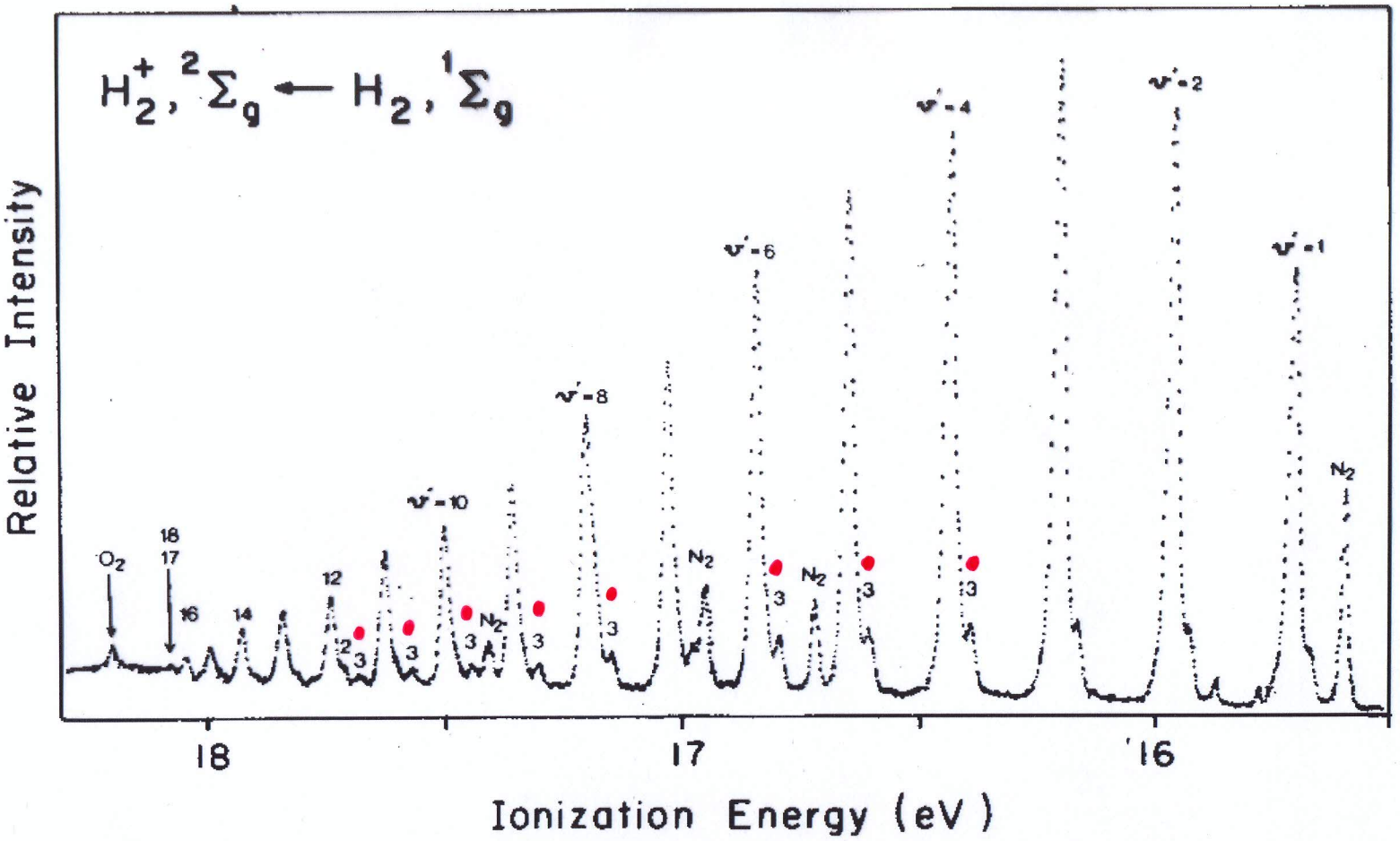

A hidrogénmolekula nagyfelbontású He(I) ultraibolya fotoelektron-spektruma. A v'=x jelzések mutatják a molekulaion rezgési kvantumszámát (a v'=0 sáv kívül esik az ábrán). 3 a J''=3 → J'=3 forgási átmenetet jelzi. A J''=0 → J'=0, J''=1 → J'=1 és a J''=2 → J'=2 forgási átmenetek nem felbontottak [i].

[i] J. Wayne Rabalais; *Principles of Ultraviolet Photoelectron Spectroscopy*, John Wiley & Sons, New York, 1977

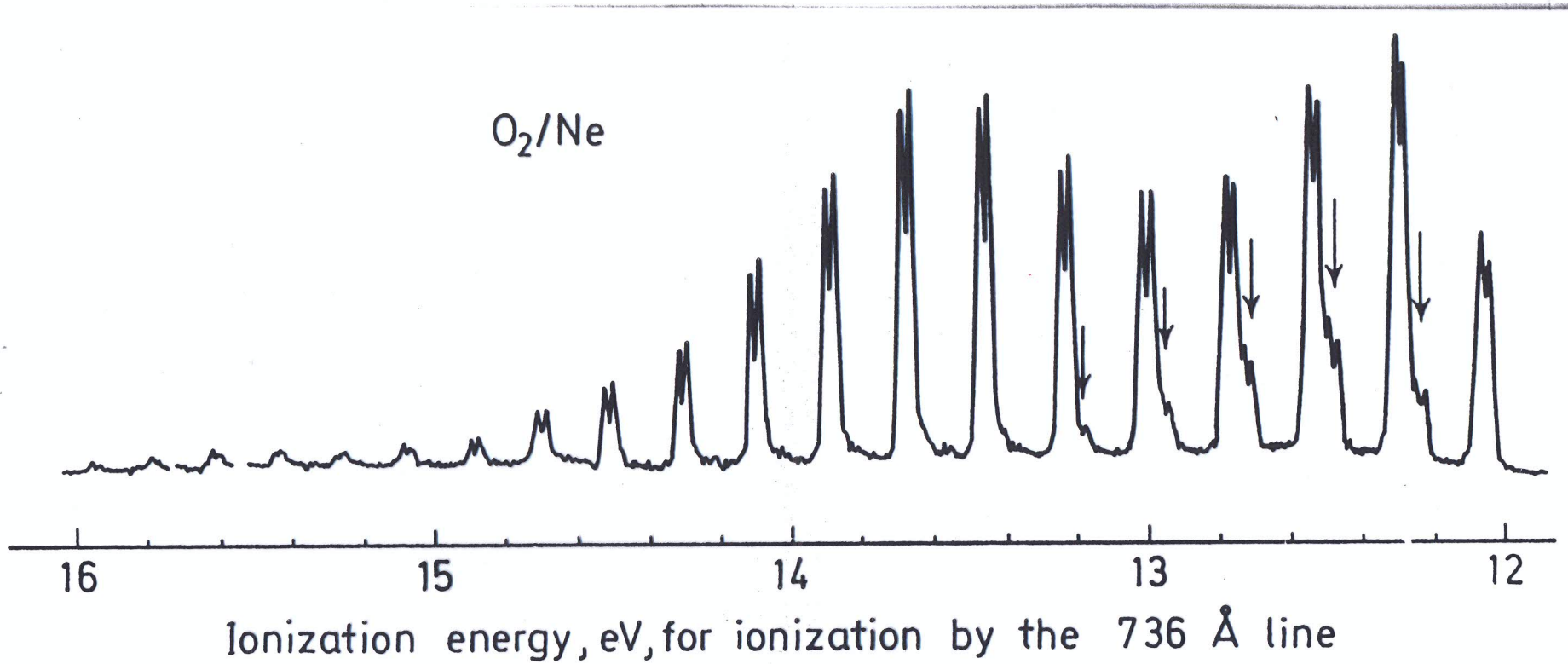

Figure 3.3. $^2\Pi_g$ band in the photoelectron spectrum of oxygen excited by neon resonance radiation, to be compared with *Figure 1.6*. The extensive vibrational structure is due to autoionization caused by the strong neon line at 736 Å. The weaker line at 744 Å gives only normal direct ionization, producing the peaks marked with arrows. The doublet structure of the peaks is due to spin–orbit coupling. (By courtesy of Professor W. C. Price)

Appendix VII. Jahn–Teller Active Vibrations and Accessible Subgroup Geometries for Degenerate States of Molecules Belonging to the Most Common Point Groups.

Parent Point Group	Jahn–Teller Active vibrations	Electronic States Split	Accessible Subgroup Geometries
D_{2d}	b_1	E	D_2
	b_2	E	C_{2v}
C_3	e	E	C_1
C_{3v}	e	E	C_1, C_s
C_{3h}	e'	E', E''	C_s
D_3	e	E	C_1, C_2
D_{3h}	e'	E', E''	C_s, C_{2v}
D_{3d}	e_g	E_g, E_u	C_i, C_{2h}
C_4	$2b$	E	C_2
C_{4v}	b_1	E	C_{2v}
	b_2	E	C_{2v}
C_{4h}	$2b_g$	E_g, E_u	C_{2h}
D_4	b_1	E	D_2
	b_2	E	D_2

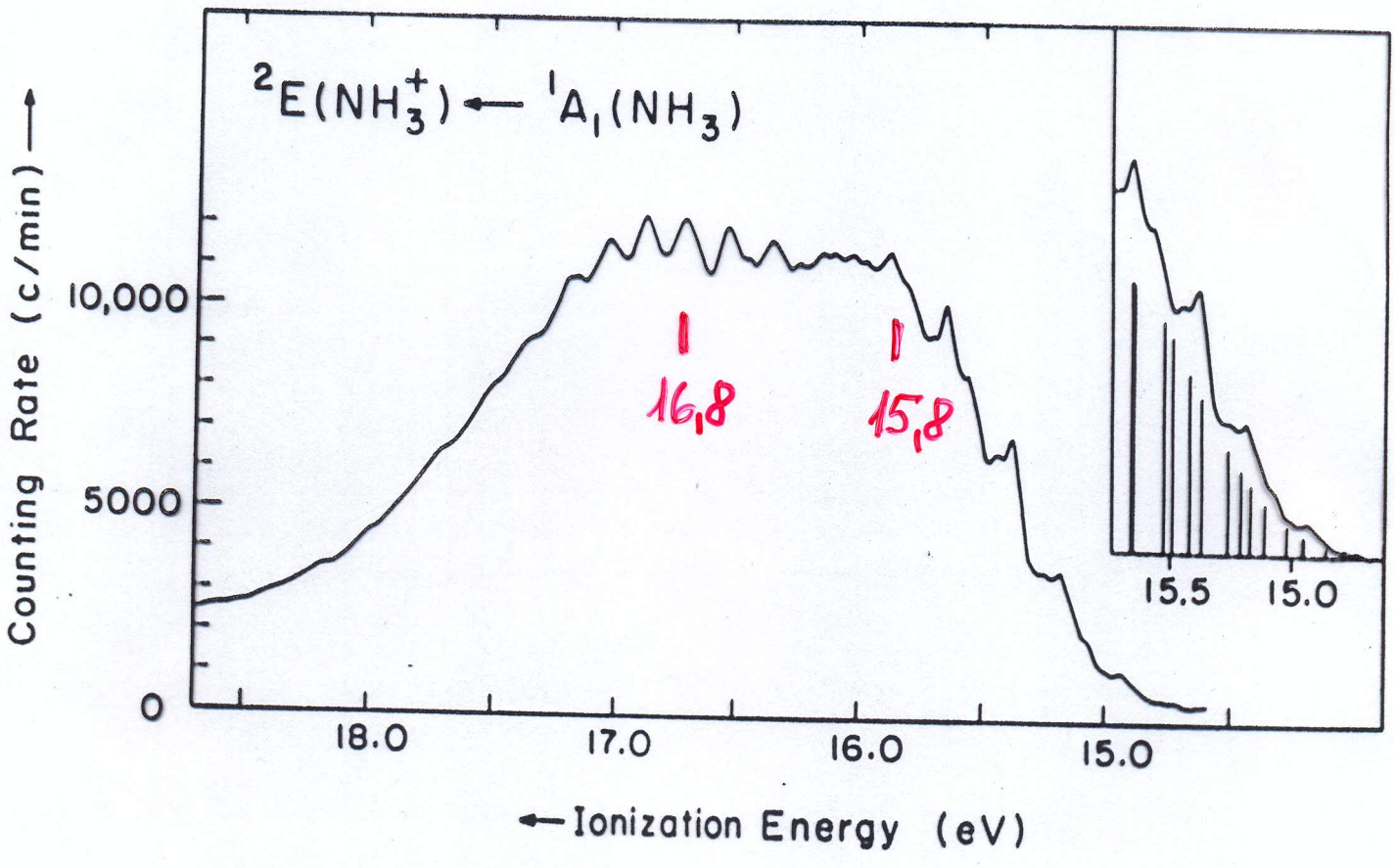
$^2E(NH_3^+) \leftarrow {}^1A_1(NH_3)$
Counting Rate (c/min)
10,000
5000
0
16,8
15,8
18.0
17.0
16.0
15.0
15.5
15.0
Ionization Energy (eV)

(24) NH_3 Ammonia

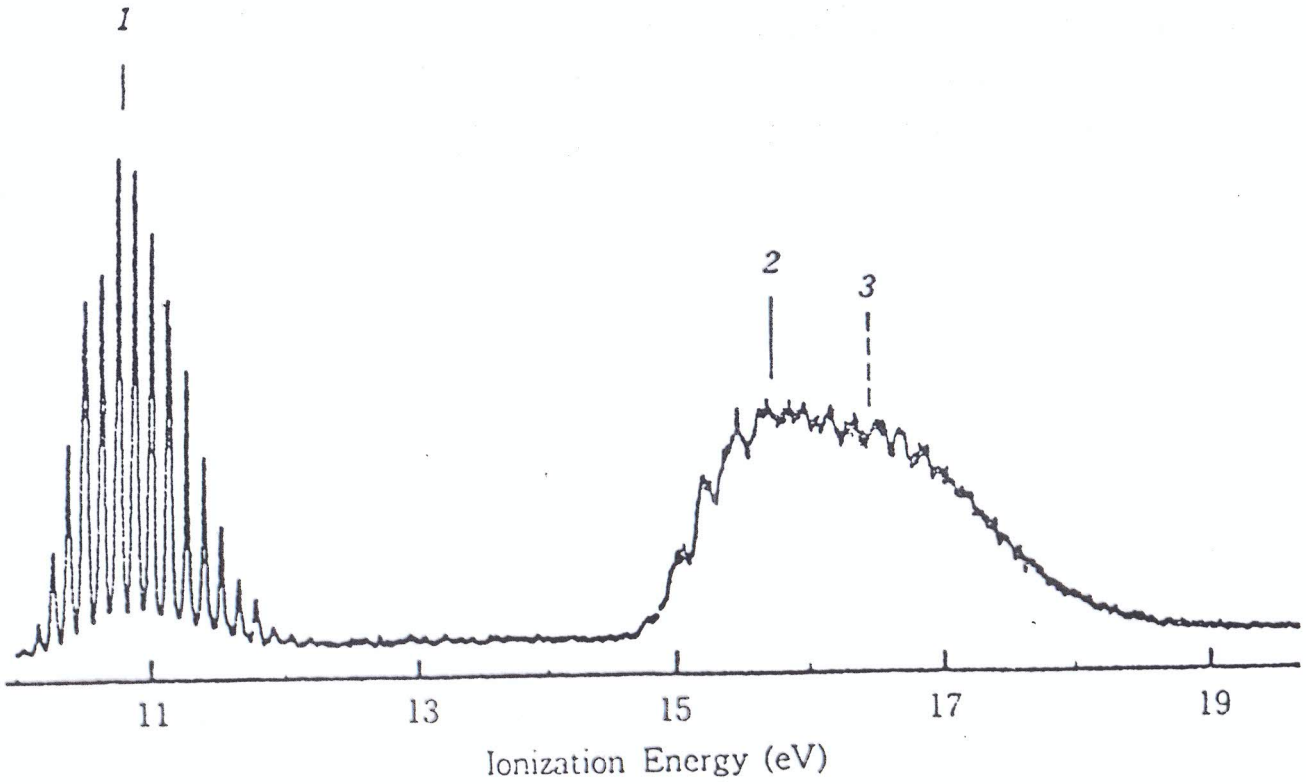

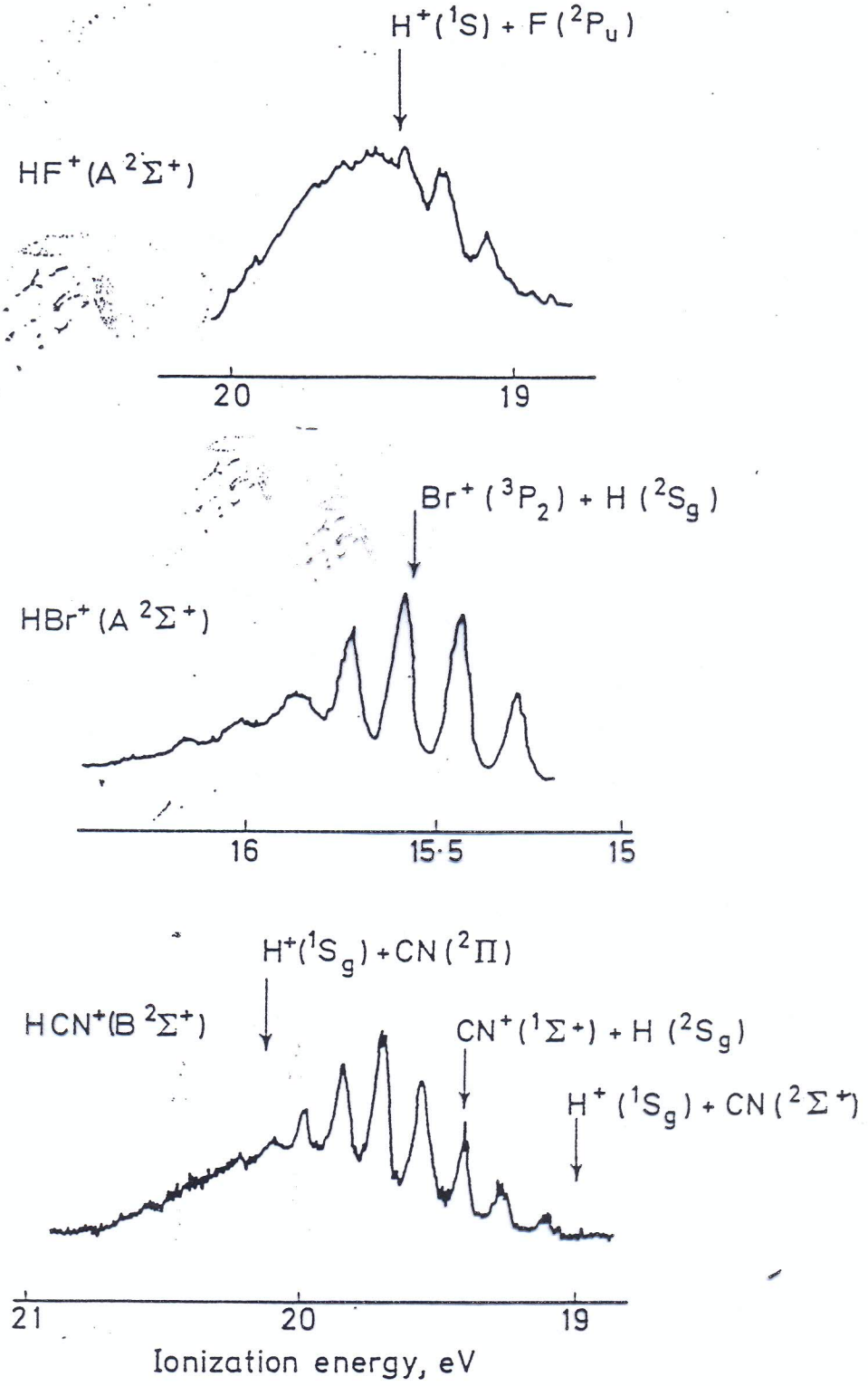

Figure 7.3. Three photoelectron bands which show broadening due to rapid dissociation. The arrows give the positions of dissociation limits for formation of the products named. (HF from Brundle[16], by courtesy of the North Holland Publishing Company; HBr from Schneider and Smith[18], by courtesy of the North Holland Publishing Company; HCN from Baker and Turner[20], by courtesy of the Council of the Royal Society)

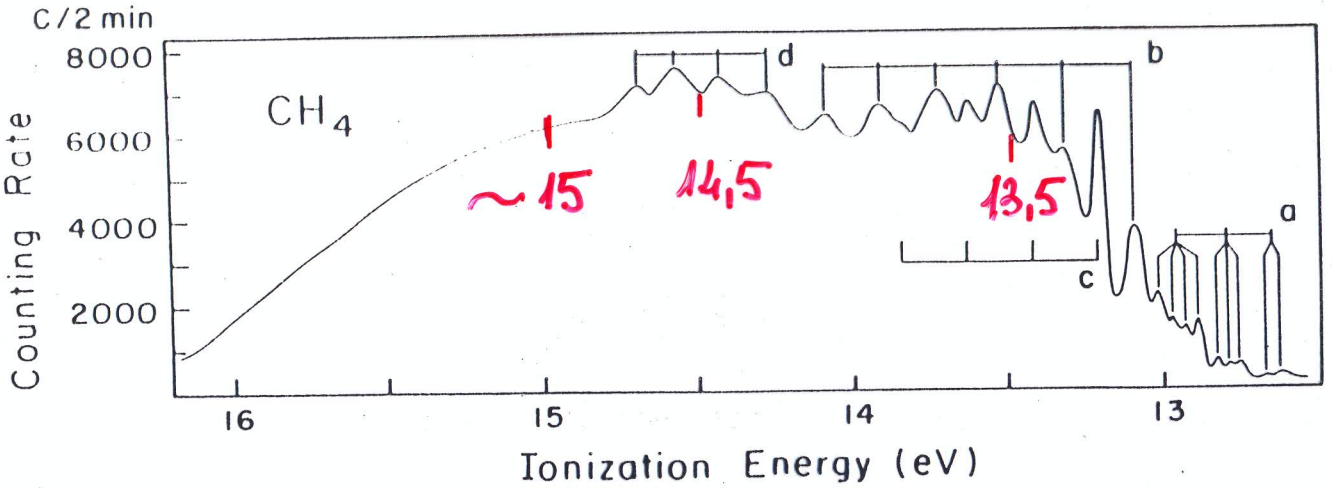

Fig. 9.2. He I spectrum of the $(1a_1^2 2a_1^2 1t_2^5)^2T_2 \leftarrow (1a_1^2 2a_1^2 1t_2^6)^1A_1$ transition of methane. Vibrational progressions are indicated by lines in the spectrum. Reproduced with permission from Ref. 23.

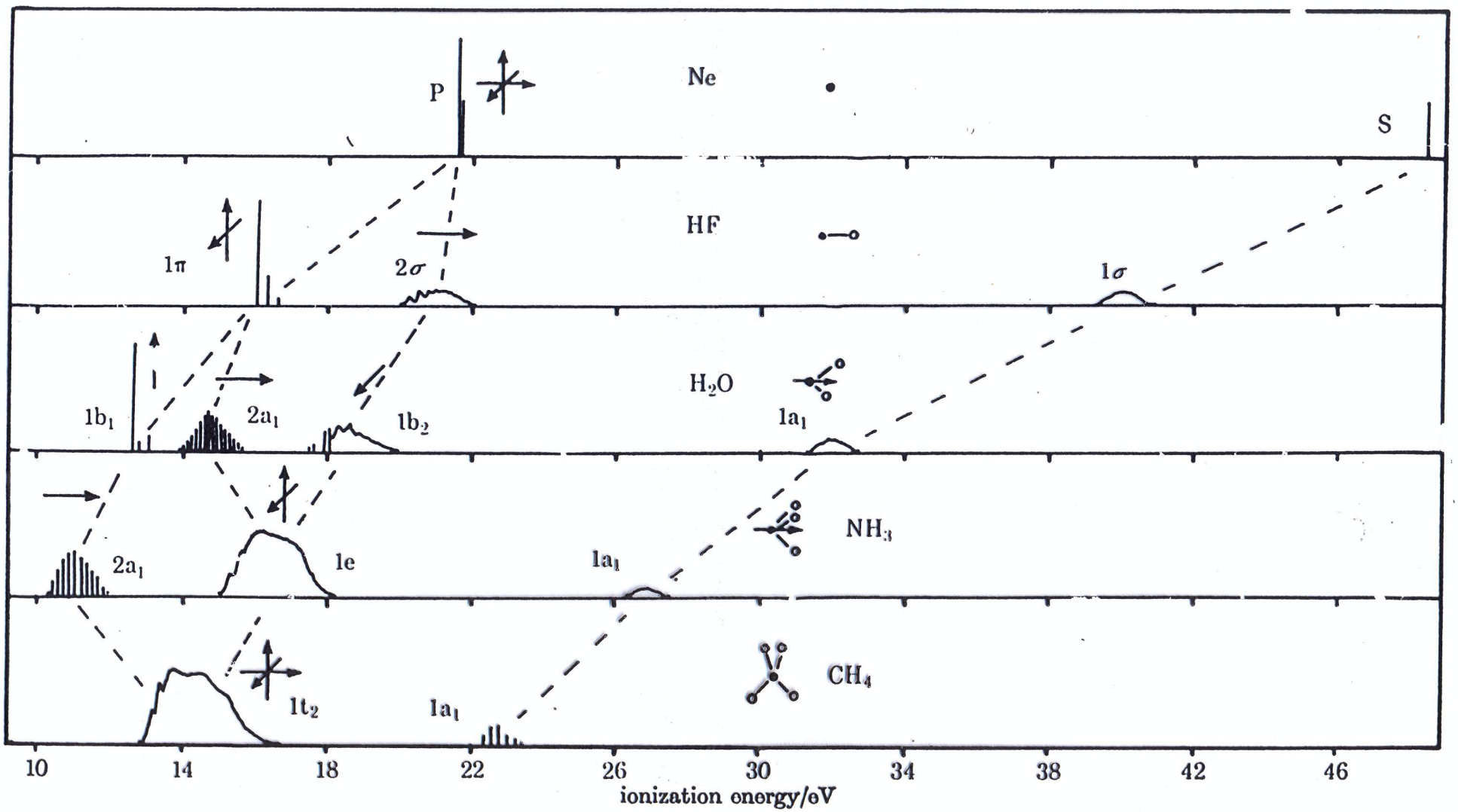
P
Ne
S
HF
1π
2σ
1σ
H2O
1b1
2a1
1b2
1a1
NH3
2a1
1e
1a1
CH4
1t2
1a1
10
14
18
22
26
30
34
38
42
46
ionization energy/eV

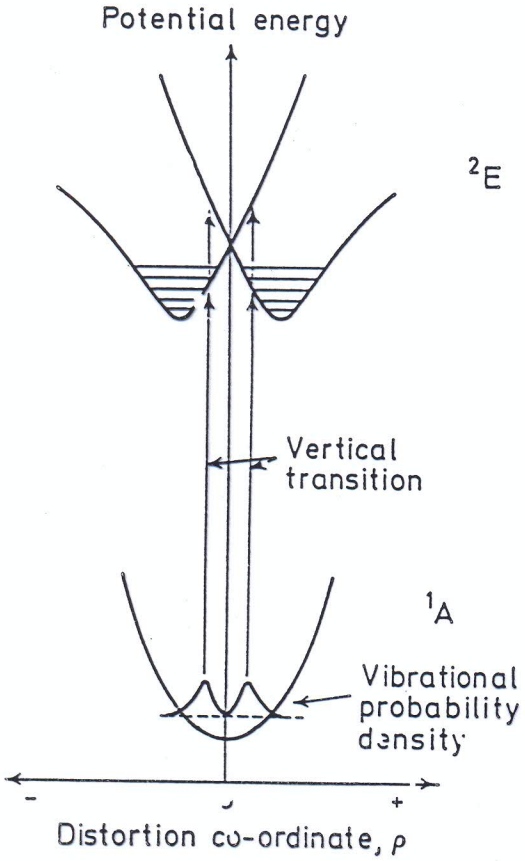

Figure 6.9. Section through the potential energy surfaces involved in a transition from a simple ground state to a ^2E ionic state undergoing a static Jahn–Teller effect

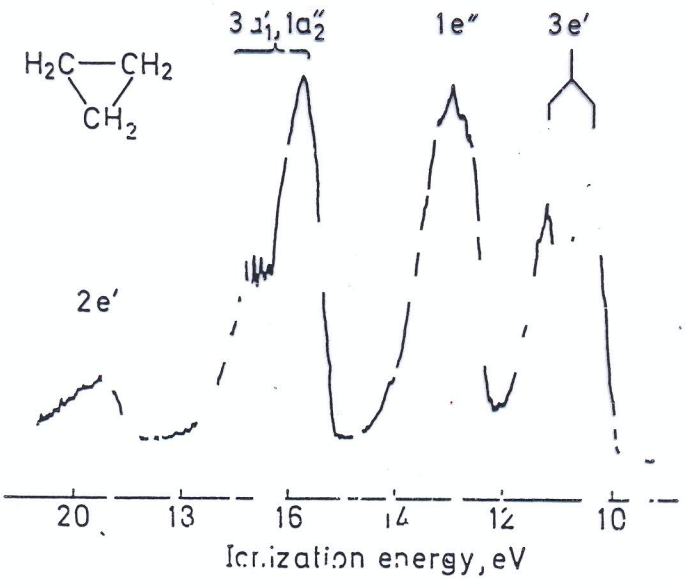

Figure 6.10. The He I photoelectron spectrum of cyclopropane showing Jahn–Teller splitting in the $3e'^{-1}$ ionization band. The $1e''^{-1}$ and $2e'^{-1}$ ionizations cause much smaller Jahn–Teller splittings, which are not apparent in the spectrum. The relative band intensities are apparently distorted by the effects of autoionization at 584 Å, since they are completely different in the spectrum taken with He II radiation[13]
(From Evans *et al.*[14], by courtesy of Elsevier Publishing Company)